

A Stochastic Multi-scale Model for Predicting the Thermal Expansion Coefficient of Early-age Concrete

S. Liu¹, X. Liu², X. F. Guan³, P.F. He¹, Y. Yuan²

Abstract: Early performance of mass concrete structures is very sensitive to the thermal expansion characteristics of concrete. As a kind of multi-phase composite, concrete has different material composition and microscopic configuration in different scales. Its thermal expansion coefficient (CTE) depends not only on the physical and mechanical properties of the constituents, but also on their distribution. What's more, CTE is also time-dependent with the procedure of hydration. This research proposes a stochastic multi-scale model for analyzing CTE of concrete. In the developed model, concrete macro-scale is divided into three different levels: cement paste scale, mortar scale and concrete meso-scale; a specific representative element volume (REV) is described by introducing stochastic parameters; and the asymptotic expansion theory is employed to realize the connection between different scales. Then, by a comparison study with experimental results and Rosen-Hashin bounds at mortar scale, the effectiveness of this model has been validated. And, the influence of aggregate's type and volume fraction on CTE of concrete is further investigated. The analysis results show that the proposed model can effectively estimate the CTE of concrete at early-age through taking the influence of material composition and configuration into consideration.

Keywords: Early-age concrete; CTE; Multi-scale; Asymptotic expansion; Stochastic

1 Instruction

In the construction of mass concrete structures, such as dam, immersed tunnel, basement, and wharf, crack control at early-age has been one of the very important aspects [Wang (1997); Zhu (1999)]. The increase of the temperature due to

¹ Institute of Applied Mechanics, Tongji University, Shanghai, China.

² Department of geotechnical engineering, Tongji University, Shanghai, China.

³ Department of Mathematics, Tongji University, Shanghai 200092, China.

Corresponding author. Email: Xian.liu@tongji.edu.cn

the exothermic nature of hydration, followed by non-uniform cooling to ambient temperature, will lead to formation of temperature gradients in concrete. These temperature gradients and resulting non-uniform thermal deformations within the element are responsible for the buildup of considerable thermal stresses, which are recognized as one of the main reasons for cracks at early-age [Ballim and Graham (2004); Abdulrazeg and Noorzaei (2010)]. In response to this mechanism, a temperature-stress coupling model has been established on macro-scale, based on heat conduction theory and continuum mechanics; besides, to solve this problem, related numerical analysis has been conducted using finite element method [Ilc and Turk (2009); Noorzaei and Bayagoob (2009)]. This macroscopic model depends on related experimental means, assuming that the CTE of concrete is a constant. However, some researchers suggest that CTE of concrete changes dramatically at early-age along with the hydration, which is not a constant [Bazant (1970); Sellevold and Bjøntegaard (2006); Grasley and Lange (2007)]. In addition, it shows that the early-age effects of mass concrete structure are very sensitive to the thermal expansion characteristics of concrete [Amin and Kim (2009); Azenha and Faria (2009); Briffaut and Benboudjema (2011)]. Therefore, it is necessary to establish a more accurate model, which can completely reflect the development of CTE at early-age and take composition and microscopic constitution of concrete into consideration.

The existing research on thermal expansion characteristics of concrete is mainly focus on test. Due to the autogenous shrinkage phenomenon, a rapid heating or cooling method is used in many tests for CTE of early-age cementitious material [Maruyama and Teramoto (2011); Yeon and Choi (2013)], thus, it ignores the additional deformation caused by autogenous shrinkage. Therefore, it's highly specialized, difficult and expensive to measure the CTE at early-age accurately; besides, due to random distribution of aggregates and other factors, the dispersion of the test result is often too large to ignore [Cusson and Hoogeveen (2006); Ozawa and Morimoto (2006)].

The basic reasons of these problems mentioned above are that, as a kind of multi-phase composite, concrete consist of cement and aggregates, it's thermal expansion characteristics depend not only on the performance of constituents, but also on their distribution with randomness; besides, along with the hydration reaction of cement, it shows significant time variability. Multi-scale mechanics provides a new approach to solve these problems, which divide concrete into different scales and think that it has different composition and microscopic constitution within different scales, and connect each scale with a certain method, called homogenization [Constantinides and Ulm (2004)]. Following this approach, some scholars realize the homogenization between scales using micro-mechanics of composites

[Schapery (1968); Rosen and Hashin (1970); Siboni and Benveniste (1991)], however, some assumptions have been made to simplify the calculation, which can't reflect the random configuration of concrete, while, as a typical non-homogeneous composite, its CTE is based not only on the thermal and mechanical properties of each components, but also on micro-constitution. In order to take this characteristic into consideration, multi-inclusion unit cell models that contain a number of randomly positioned and, where applicable, randomly oriented spherical, spherical or cylindrical discontinuous reinforcements have been studied [Bohm and Han (2004)]; then, 3D reconstruction technology of X-ray computed tomography (CT) has been introduced to the modeling of concrete composites at the meso-scale [Du and Jiang (2011)]. While, for theory of computation, asymptotic expansion theory has been proposed [Kesavan (1979); Cui and Cao (1998)], which is applicable to the composite materials of periodic or random structure with high inclusion content, and take the interaction between inclusions into consideration well [Yang and Cui (2012); Li and Cui (2004); Feng and Cui (2004)].

In this research, concrete has been divided into three different scales firstly, according to the scale law. In each scale, a corresponding representative element volume (REV) is described. Then, the connections between different scales are successfully realized using asymptotic expansion method. Thus, a stochastic multi-scale model for CTE of early-age concrete is proposed; a comparison study with experimental results and Rosen-Hashin bounds at mortar scale is conducted, which validated the effectiveness of presented model, and, the influence of aggregate's type and volume fraction on CTE of concrete is further investigated.

2 Representation

As a kind of multi-phase composite, concrete has different material composition and microscopic configuration in different scales; besides, along with the hydration reaction of cement, the performance of concrete shows significant time variability. Therefore, to calculate the CTE in a more accurate way, in this research, macro-scale has been divided into concrete meso-scale, mortar scale, cement paste scale, according to the scale law, as shown in Fig. 1.

Since there is no influence of randomly distributed aggregates and the experiment on cement paste scale is easy to operate with high precision, cement paste is regarded as isotropic and homogeneous, and, its thermal and mechanical parameters are obtained through test.

Mortar scale is a two-phase composite consists of cement paste as matrix and sand as inclusion. With randomly distributed sand, a simple RVE is usually insufficient in providing reliable estimates of the performance of mortar. So, a specific

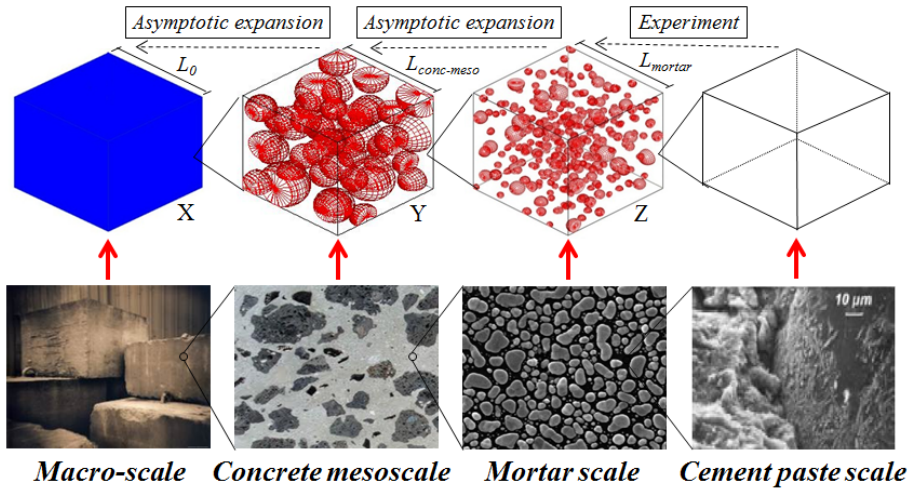


Figure 1: Scale division of concrete

REV needs to be described, each one is further assumed to consist of matrix and sphere which is non-overlapping and distributed randomly, as shown in Fig.1; each sphere is defined by four parameters, they are center position (y_1^n, y_2^n, y_3^n) and diameter D_{sand} of sphere. With regard to this specific REV for mortar, the size of it L_{mortar} is $0.5 - 1cm$, diameter of sphere is $100 - 500\mu m$; besides, it's remarkable that the center position and D_{sand} are subject to uniform distribution within their own range. Thus, the REV is further described with stochastic parameters, which can significantly simulate the randomness and uniformity of sand's distribution in cement paste.

And, concrete meso-scale is composed of equivalent homogeneous mortar as matrix and coarse aggregate as inclusion, also identified as a two-phase composite. A specific REV which can significantly simulate the randomness and uniformity of coarse aggregate's distribution in cement paste needs to be described the same way as mortar scale, in which sphere is also non-overlapping and distributed randomly, as shown also in Fig. 1. With regard to this specific REV for concrete meso-scale, the size of it $L_{conc-meso}$ is $5 - 10cm$, diameter of sphere is $0.5 - 1cm$. And, the center position and $D_{aggregate}$ are also subject to uniform distribution within their range.

Because of $D_{sand} \ll L_{mortar} \leq D_{aggregate} \ll L_{conc-meso} \ll L_0$, where L_0 characterizes the macro-scale, the requirement of separation of scales is satisfied. The time variability of cement paste plays an important role in the thermal and mechanical performance development of concrete at early-age, while the properties

of sand and aggregated is constant. So, based on the experiment of cement paste, the connection between different scales is successfully established by asymptotic expansion theory.

3 A stochastic multi-scale model for CTE of concrete

3.1 Governing equations

A point of homogeneous body can be treated as a periodic multiple permutation of REV which is heterogeneous in the asymptotic expansion theory, as shown in Fig. 2, when the equivalent homogeneous body is subjected to external forces, its field quantities such as displacement, stress and strain, will vary within the global coordinate x , in the meantime, because of the high heterogeneity of local constitution, they will also vary rapidly within coordinate y and z . Therefore, following the multi-scale representation of concrete, the scale factor $\epsilon_{conc-meso}$ at the concrete meso-scale is defined as $\epsilon_{conc-meso} = \epsilon$, in which ϵ denote the basic scale factor. At the mortar scale, the scale factor ϵ_{mortar} is defined as $\epsilon_{mortar} = \epsilon^2$. For the sake of simplicity, probability distributions $w^{conc-meso}$ and w^{mortar} can be denoted as w with $w = \{w^{conc-meso} : y \in Y; w^{mortar} : z \in Z\}$.

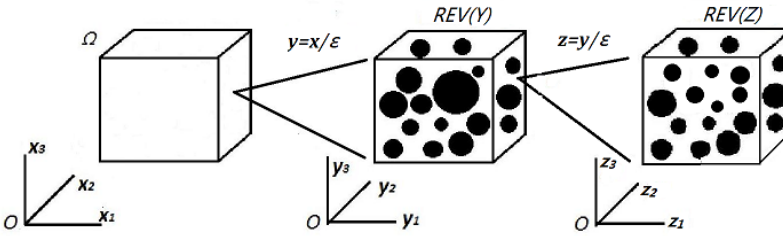


Figure 2: Representation of multi-scale method

It should be realized that the thermal expansion performance is a kind of thermal-mechanical coupling behavior; coefficient of thermal expansion connects the mechanical and thermal behavior, which can be described as following [Feng and Cui (2004)]:

$$\frac{\partial}{\partial x_j} \left[C_{ijkl}^\epsilon(x) \left(\frac{1}{2} \left(\frac{\partial u_k^\epsilon(x)}{\partial x_l} + \frac{\partial u_l^\epsilon(x)}{\partial x_k} \right) - a_{kl}^\epsilon(x) \theta^0(x) \right) \right] = f_i(x), x \in \Omega \quad (1)$$

Where $C_{ijkl}^\epsilon(x)$ and $a_{kl}^\epsilon(x)$ is the stiffness and thermal expansion coefficients; $u^\epsilon(x)$ represent the displacement vector corresponding to point x of equivalent homogeneous body; $\theta^0(x)$ is the homogeneous temperature field; $h(x)$ is the heat produced

by internal heat sources per unit time and unit mass, while $f_i(x)$ is the internal force. The boundary conditions are specified as follows:

$$\theta^\varepsilon(x) = \bar{\theta}(x), x \in \Gamma_1 \quad ; \quad u_i^\varepsilon(x) = \bar{u}_i(x), x \in \Gamma_2 \tag{2}$$

Γ_1 is the temperature boundary and Γ_2 is the displacement boundary, while $\bar{\theta}(x)$ and $\bar{u}(x)$ denote the corresponding boundary conditions.

3.2 Multi-scale analysis

Considering not only the homogeneous mechanical behaviors but also the local configuration of material, let $x \ y \ z$ denote the coordinate system of the macro-scale, the concrete meso-scale and the mortar scale, respectively. They are related one another as follows:

$$y = x/\varepsilon; z = y/\varepsilon \tag{3}$$

Besides, the properties of material composition in REV can be expressed as:

$$C_{ijkl}^\varepsilon(x) = C_{ijkl}(y, w^1) = C_{ijkl}(y, z, w) \tag{4}$$

$$a_{kl}^\varepsilon(x) = a_{kl}(y, w^1) = a_{kl}(y, z, w) \tag{5}$$

An asymptotic expansion of $u^\varepsilon(x)$ is formed with coordinate $x \ y$ and z :

$$u^\varepsilon(x) = u^0(x) + \varepsilon u^1(x, y, z) + \varepsilon^2 u^2(x, y, z) \tag{6}$$

Differentiation with respect x defined as:

$$\frac{\partial}{\partial x_i} = \frac{\partial}{\partial x_i} + \varepsilon^{-1} \frac{\partial}{\partial y_i} + \varepsilon^{-2} \frac{\partial}{\partial z_i} \tag{7}$$

Substituting Eq.6 and Eq.7 into Eq.1 and letting $\varepsilon \rightarrow 0$, the coefficients of same powers $\varepsilon^n (n = -4, -3, -2, -1)$ must be zero. The following partial differential equation is determined from the ε^{-4} :

$$\frac{\partial}{\partial z_j} \left(C_{ijkl}(y, z, w) \frac{\partial u_k^0}{\partial z_l} \right) = 0 \tag{8}$$

Since u^0 is only a function of x , the above relation is automatically satisfied. The following partial differential equation is determined from the ε^{-3} :

$$\frac{\partial}{\partial y_j} \left(C_{ijkl}(y, z, w) \frac{\partial u_k^0}{\partial z_l} \right) + \frac{\partial}{\partial z_j} \left(C_{ijkl}(y, z, w) \left(\frac{\partial u_k^0}{\partial y_l} + \frac{\partial u_k^1}{\partial z_l} \right) \right) = 0 \tag{9}$$

Because u^0 is only a function of \mathbf{x} , the terms $\partial u_k^0/\partial z_l$ and $\partial u_k^0/\partial y_l$ vanish, thus, u^1 is a function of \mathbf{x} and \mathbf{y} , writing as follows:

$$u_i^1(\mathbf{x}, \mathbf{y}) = N_i^{kl}(\mathbf{y}) \frac{\partial u_k^0}{\partial x_l} \tag{10}$$

$N_i^{kl}(\mathbf{y})$ is 1-periodic matrix valued function defined in $REV(\mathbf{Y})$ at concrete meso-scale, which can reflect the influence of local heterogeneity of composites. Considering u^0 is only a function of \mathbf{x} , and u^1 is a function of \mathbf{x} and \mathbf{y} , the partial differential equation determined from the ϵ^{-2} can be simplified as:

$$\frac{\partial}{\partial z_j} \left[C_{ijkl}(\mathbf{y}, \mathbf{z}, \mathbf{w}) \left(\frac{\partial u_k^0}{\partial x_l} + \frac{\partial u_k^1}{\partial y_l} + \frac{\partial u_k^2}{\partial z_l} \right) \right] = 0 \tag{11}$$

The terms $\partial u_k^0/\partial x_l$ and $\partial u_k^1/\partial y_l$ are functions of \mathbf{x} and \mathbf{y} , which allows writing u^2 as follows:

$$u_i^2(\mathbf{x}, \mathbf{y}, \mathbf{z}) = M_i^{kl}(\mathbf{z}) \left(\delta_{km} \delta_{ln} + \frac{\partial N_k^{mn}}{\partial y_l} \right) \frac{\partial u_m^0}{\partial x_n} \tag{12}$$

Where δ_{ij} is the Kronecker delta, $M_i^{kl}(\mathbf{z})$ is 1-periodic matrix valued function defined in $REV(\mathbf{Z})$ at mortar scale. Substituting Eq.10 and Eq.12 into Eq.11:

$$\begin{aligned} & C_{ijkl}(\mathbf{y}, \mathbf{z}, \mathbf{w}) \left(\frac{\partial u_k^0}{\partial x_l} + \frac{\partial u_k^1}{\partial y_l} + \frac{\partial u_k^2}{\partial z_l} \right) \\ &= C_{ijkl}(\mathbf{y}, \mathbf{z}, \mathbf{w}) \left(\delta_{ks} \delta_{lt} + \frac{\partial M_k^{st}}{\partial z_l} \right) \left(\delta_{ms} \delta_{nt} + \frac{\partial N_s^{mn}}{\partial y_t} \right) \frac{\partial u_m^0}{\partial x_n} \end{aligned} \tag{13}$$

Substituting Eq.13 into Eq.11 yields the following equation, termed as the mortar scale equation for domain \mathbf{Z} , which is the controlling equation for $M_i^{kl}(\mathbf{z})$:

$$\frac{\partial}{\partial z_j} \left[C_{ijkl}(\mathbf{y}, \mathbf{z}, \mathbf{w}) \left(\delta_{ks} \delta_{lt} + \frac{\partial M_k^{st}}{\partial z_l} \right) \right] = 0 \tag{14}$$

It can be noticed that $M_i^{kl}(\mathbf{z})$ is only related to coordinate \mathbf{z} for mortar scale. The following simplified partial differential equation is determined from the ϵ^{-1} :

$$\frac{\partial}{\partial y_j} \left[C_{ijkl}(\mathbf{y}, \mathbf{z}, \mathbf{w}) \left(\frac{\partial u_k^0}{\partial x_l} + \frac{\partial u_k^1}{\partial y_l} + \frac{\partial u_k^2}{\partial z_l} \right) \right] + \frac{\partial}{\partial z_j} \left[C_{ijkl}(\mathbf{y}, \mathbf{z}, \mathbf{w}) \left(\frac{\partial u_k^1}{\partial x_l} + \frac{\partial u_k^2}{\partial y_l} \right) \right] = 0 \tag{15}$$

The volume average for the mortar scale domain \mathbf{Z} is defined as:

$$\langle \bullet \rangle_2 = \frac{1}{|\mathbf{Z}|} \int_{\mathbf{Z}} \bullet dz \tag{16}$$

Substitution Eq.13 into Eq.15 with the help of Eq.16, the following controlling equation for $N_i^{kl}(y)$ in REV(Y) at concrete meso-scale is obtained:

$$\frac{\partial}{\partial y_j} \left[C_{ijst}^{H_1}(y, w) \left(\delta_{ms} \delta_{nt} + \frac{\partial N_s^{mn}}{\partial y_t} \right) \right] = 0 \tag{17}$$

Where, $C_{ijst}^{H_1}(y, w)$ is the stiffness coefficient of homogenized mortar, denoted as:

$$C_{ijst}^{H_1}(y, w) = \frac{1}{|Z|} \int_Z C_{ijkl}(y, z, w) \left(\delta_{ks} \delta_{lt} + \frac{\partial M_k^{st}}{\partial z_l} \right) \tag{18}$$

Thus, $N_i^{kl}(y)$ can be obtained by solving Eq.18. The following partial differential equation is determined from the ϵ^0 :

$$\begin{aligned} & \frac{\partial}{\partial x_j} \left[C_{ijkl}(y, z, w) \left(\frac{\partial u_k^0}{\partial x_l} + \frac{\partial u_k^1}{\partial y_l} + \frac{\partial u_k^2}{\partial z_l} \right) \right] + \frac{\partial}{\partial y_j} \left[C_{ijkl}(y, z, w) \left(\frac{\partial u_k^1}{\partial x_l} + \frac{\partial u_k^2}{\partial y_l} \right) \right] \\ & + \frac{\partial}{\partial z_j} \left(C_{ijkl}(y, z, w) \frac{\partial u_k^2}{\partial x_l} \right) - \frac{\partial}{\partial x_j} \left(C_{ijkl}(y, z, w) a_{kl}(y, z, w) \theta^0(x) \right) = f_i \end{aligned} \tag{19}$$

The volume average for the mortar scale domain Z is defined as:

$$\langle \bullet \rangle_1 = \frac{1}{|Y|} \int_Y \bullet dz \tag{20}$$

Substitution Eq.13 into Eq.19 with the help of Eq.16 and Eq.20, the following controlling equation for concrete meso-scale is obtained:

$$\frac{\partial}{\partial x_j} \left[C_{ijkl}^H(w) \frac{\partial u_k^0}{\partial x_l} - \Psi \theta^0(x) \right] = f_i \tag{21}$$

Where, $C_{ijkl}^H(w)$ is the stiffness coefficient of the homogenized concrete meso-scale, denoted as:

$$C_{ijkl}^H(w) = \frac{1}{|Y|} \int_Y C_{ijst}^{H_1}(y, w) \left(\delta_{ks} \delta_{lt} + \frac{\partial N_s^{kl}}{\partial y_t} \right) dy \tag{22}$$

Ψ can be defined as:

$$\Psi = \int_Y \int_Z C_{ijkl}(y, z, w) a_{kl}(y, z, w) dz dy \tag{23}$$

According to the form of equation (1), Ψ can also be denoted as:

$$\Psi = C_{ijkl}^H(w) a_{kl}^H(w) \tag{24}$$

Then, the homogenized CTE is obtained as:

$$a_{kl}^H(w) = \Psi [C_{ijkl}^H(w)]^{-1} \tag{25}$$

As can be seen from the expression, homogenized CTE of concrete is not only corresponding to the stiffness coefficients $C_{ijkl}(y, z, w)$ and thermal expansion coefficients $a_{kl}(y, z, w)$ of different material composition in different scales, but also to $N_i^{kl}(y)$ and $M_i^{kl}(z)$ which reflect the influence of local heterogeneity of REV.

4 Analysis procedure

4.1 Computation of homogenized CTE

According to the REV of concrete at the mortar and the concrete meso-scale, different inclusions, such as sand and coarse aggregates, have different size and positions in different samples. From the multi-scale Eq.18 and Eq.22, it can be seen that this configuration has an influence on the stiffness of concrete, which also means on CTE. Thus, as was mentioned in the context of the description of mortar and concrete meso-scale, the characteristics of the homogenized concrete, can be evaluated by means of the proposed multi-scale model.

The procedure for determination of the thermal expansion properties of the homogenized concrete with randomly distributed inclusions can be summarized as follows:

- Based on the statistical characteristics of mortar scale, for a random distribution w_s^{mortar} , a sample is generated. Then, Eq.14 is solved in REV (Z) to obtain $M_i^{kl}(z, w_s^{mortar})$. Thereafter, the homogenized elastic tensor $C_{ijst}^{H_1}(y, w_s^{mortar})$, corresponding to sample w_s^{mortar} , is computed by means of Eq.18.
- Analogous to (1), for a random distribution $w_s^{conc-meso}$ at the concrete meso-scale, a sample is generated. Then, Eq.17 is solved in REV (Y) to obtain $N_i^{kl}(y, w_s^{conc-meso})$. Thereafter, the homogenized elastic tensor $C_{ijkl}^H(w_s^{mortar}, w_s^{conc-meso})$, corresponding to sample $w_s^{conc-meso}$, is computed by means of Eq.22.
- According to Eq.23 to Eq.25, with the help of $C_{ijkl}^H(w_s^{mortar}, w_s^{conc-meso})$, the homogenized CTE $a_{kl}^H(w_s^{mortar}, w_s^{conc-meso})$ is obtained.
- Following the generation of T samples with random distributions $w_s = \{w_s^{conc-meso} : y \in Y; w_s^{mortar} : z \in Z\}$, $s = 1, 2, \dots, T$, and based on the Kolmogorov's strong law of large numbers, the expected-homogenized CTE $\hat{a}_{ij}(x)$ representing the homogenized material can be computed with the help of the equation:

$$\hat{a}_{ij}(x) = \frac{\sum_{s=1}^T a_{kl}^H(w)}{T}, T \rightarrow \infty \quad (26)$$

4.2 Flowchart of multi-scale algorithm

The flowchart of the algorithm for the proposed multi-scale method for prediction of the thermal expansion properties of concrete is given as follows:

Table 1: Flowchart for computing the thermal expansion properties of concrete

Input		$E_{cement-paste}, a_{cement-paste}; E_{sand}, a_{sand};$ Diameter distribution of sand $D_{sand};$ volume fraction of sand $f_{sand}; E_{aggregate}, a_{aggregate};$ Diameter distribution of coarse aggregate $D_{aggregate};$ volume fraction of coarse aggregate $f_{aggregate}$
Mortar scale	(1)	Generate a sample REV (Z) with a random distribution w_s^{mortar} , which consist of cement paste as matrix and sphere which distributed randomly and simulate sand inclusion, as shown in Fig.1; establish the finite element model for it with 10-nodes tetrahedron elements, as shown in Fig. 3
	(2)	Compute $M(z)$ by solving Eq.14; and evaluate elastic tensor $C_{ijst}^{H_1}(y, w)$ of homogenized mortar from Eq.18
Concrete meso-scale	(3)	Generate a sample REV (Y) with a random distribution $w_s^{conc-meso}$, which consist of homogenized mortar as matrix and sphere which distributed randomly and simulate sand inclusion, as shown in Fig.1; establish the finite element model for it with 10-nodes tetrahedron elements.
	(4)	Compute $N(y)$ by solving Eq.17; and evaluate elastic tensor $C_{ijst}^H(y, w)$ of homogenized concrete meso-scale from Eq.22
	(5)	Compute homogenized coefficient of thermal expansion $a_{kj}^H(w)$ according to Eq.23-25
Macro-scale	(6)	Based on the Kolmogorov’s strong law of large numbers, the expected-homogenized CTE $\hat{a}_{ij}(x)$ representing the homogenized material can be computed by Eq.26
Output		$C_{ijst}^{H_1}(y, w), C_{ijst}^H(y, w), \hat{a}_{ij}(x)$

5 Model validation

So far, the homogenized CTE of early-age concrete could be evaluated based on the following main assumptions: (a) concrete is considered as a three-scale composite medium, composed of cement paste and sand of the mortar scale, and homogenized mortar and coarse aggregate of the concrete meso-scale, homogenized to an isotropic continuum of the macro-scale; (b) the heterogeneous micro-scale and meso-scale structures are modeled by periodic REV.

The multi-scale formulations described in Section 3 could be implemented with the aid of finite element method. Typical finite element meshes employed in the present study are shown in Fig. 3.

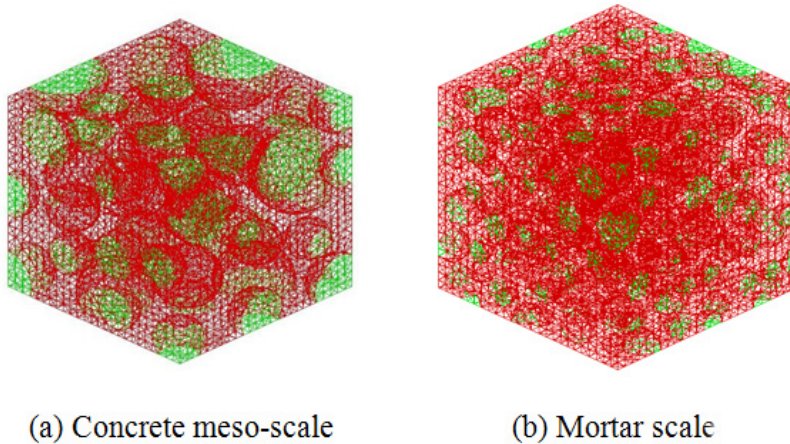


Figure 3: The entire FEM model of REV

The main purpose of this section is to verify the capability of the proposed multiscale technique to determine CTE of early-age concrete. The validation work of the developed model hereafter will be conducted at the mortar scale considering the available experimental results in the open literature. The predictive capacities of the model will then be shown by calculating the CTE values and comparing them with corresponding experimentally determined values.

A comparison study with experimental results [Wyrzykowski and Lura (2013)] and Rosen-Hashin bounds is conducted hereafter. The employed thermal and mechanical properties of sand are shown in Tab. 2.

Table 2: Thermal and mechanical properties of sand

E(Gpa)	Poisson's ratio	CTE(um/m/0c)	Volume fraction(%)
60	0.2	9	40

From the comparison with experiment results shown in Fig. 4. Firstly, the lower values of the CTE observed for mortar than for the cement pastes are due to the lower, constant CTE of sand, which consequently restrain the deformation of the

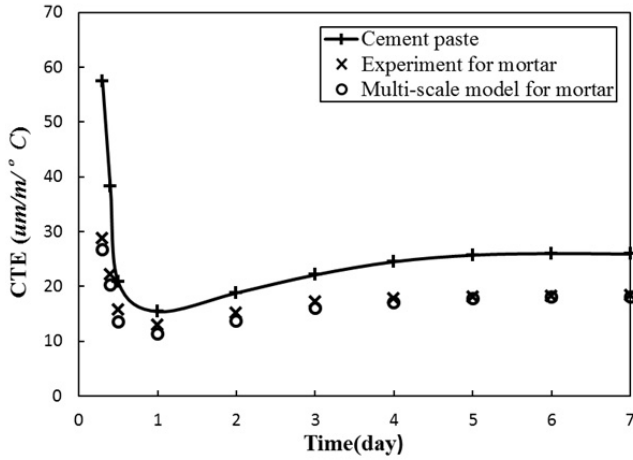


Figure 4: Comparison of multi-scale model and experiment for CTE

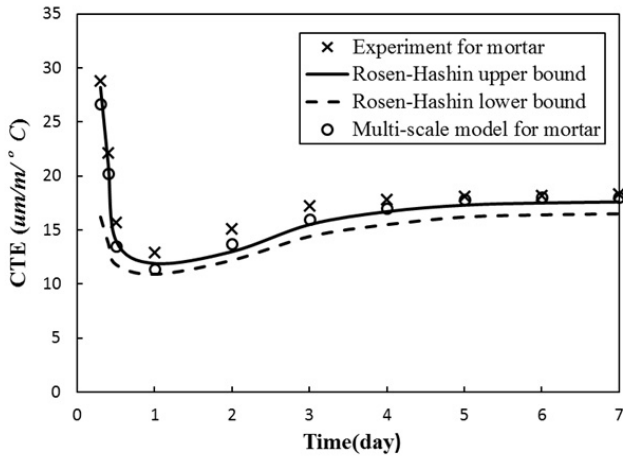


Figure 5: Comparison of multi-scale model and Rosen-Hashin bounds for CTE

paste, however, the trend of them are same. Secondly, it is observed that the CTE of cement paste is rapidly reduced at the beginning, and then grow slowly after minimum value is reached until stationary. It can be explained that, before initial set, since the solid skeleton have not been formed and liquid phase with high CTE account for the main portion, the CTE of cement paste is high; as cement paste reaches final set, free water content decreases rapidly, solid skeleton gradually formed, and modulus of elasticity also enhance significantly, the CTE reaches a minimum; then, with the hydration of cement, an increase of temperature leads an increase of internal relative humidity in pores and the resulting additional deformation acts in the same direction as the pure thermal dilation, thus an additional expansion is induced by an increase of temperature, expressed as higher CTE; however, along with the growth of age, the solid skeleton is basically not changed, and hydration reaction rate reduce, CTE becomes stable.

As shown in Fig.5, a comparison with experiment and Rosen-Hashin bounds is performed. First of all, it can be seen that the calculation results of proposed model are in good agreement with experimental data. Secondly, for these two models, the results are slightly lower of experiment. On the one hand, it is on account of that such models are based on a series of simplified assumptions, one of the main assumptions is that mortar is regarded as sand dispersed in the homogenous cement paste with perfect bond between them, the other one is the assumed no influence of micro-cracking on the stiffness. On the other hand, in the experiment, some air with high CTE may have been entrapped between the membrane and the briquette which can result in measurement error [24]. So, take all the factors into consideration, a good agreement between the predictions and the experimental data was obtained in this study, thus, it can conclude that the proposed model in this research is quiet effective.

6 Discussion

In previous section, the cement paste scale and mortar scale has been connected effectively using proposed model. In this section, based on the computation results on mortar scale, a cross-scale study at CTE of early-age concrete is performed, and the influence of aggregate's type and volume fraction are further investigated.

Three kinds of normally used representative aggregates are chose: siliceous aggregate (quartzite), igneous aggregate (granite), and calcareous aggregate (limestone), thermal and mechanical properties of these aggregates are shown in Tab. 2 [Chang and Zhang (2007); Bazant and Kaplan (1996)], the volume fraction is about 20%-40% .

As shown in Fig. 6, CTE of concrete for different kinds of aggregates at volume

Table 3: Thermal and mechanical properties of coarse aggregate

	E(Gpa)	Poisson's ratio	CTE($\mu\text{m}/\text{m}^{\circ}\text{C}$)
quartzite	17.9-69.3	0.17-0.36	10.3
granite	29.8-61.1	0.12-0.27	6.8
limestone	21.4-84.2	0.18-0.35	5.5

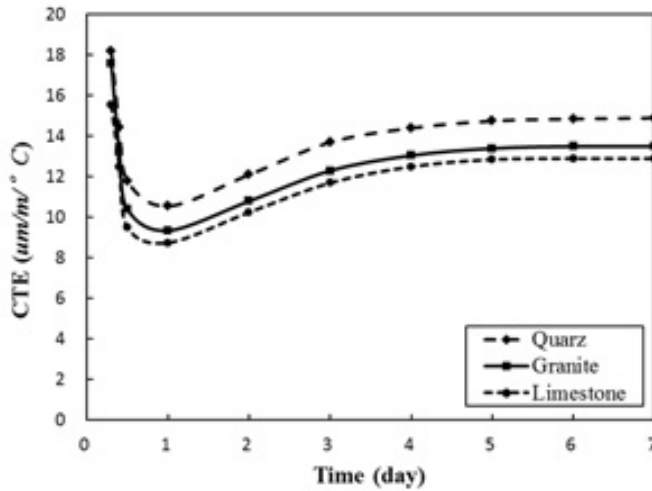


Figure 6: CTE of concrete for different kinds of aggregates at volume fraction 35%

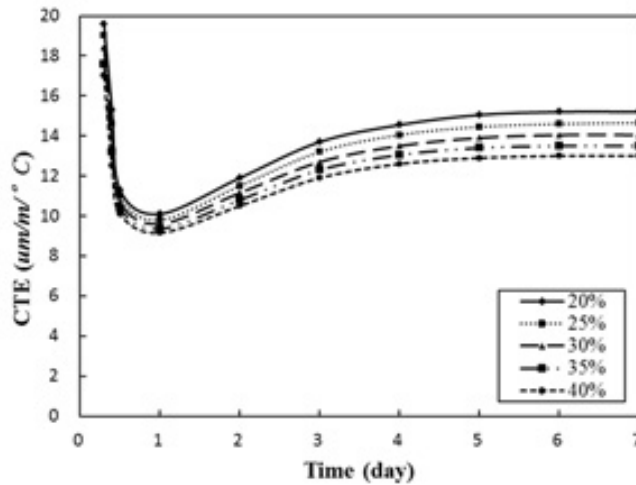


Figure 7: CTE of concrete with granite aggregate at different volume fraction

fraction 35% are compared. Firstly, CTE of concrete with different kinds of aggregates share the same trend, which is determined by the mortar matrix; secondly, whether in the sharp decline or slow growth period of CTE at the early-age, the CTE of concrete with calcareous aggregate (limestone) is obviously lower than concrete with siliceous aggregate (quartzite), while concrete with igneous aggregate (granite) fall in between these two. Gradually stabilized in the CTE, it reduced by 17.2% relative to the mortar matrix for concrete with quartzite, while 25% and 28.3% for granite and limestone respectively. Thus, it can conclude that aggregate's type have important influence on CTE of concrete at early-age.

As shown in Fig 7, CTE of concrete with granite aggregate are chose as an example to study the influence of aggregate's volume fraction. As the volume fraction of aggregate increases, a relative lower CTE of concrete is observed, while the trends stay the same. The main reason is that, concrete meso-scale is considered as a two-phase material with effective homogeneous mortar as matrix and coarse aggregate as inclusions, when temperature changes, different thermal deformation occurs between aggregate and mortar matrix due to different CTE, since this mismatch in thermal deformation, internal restraint exists between randomly distributed aggregates and mortar matrix, which consequently restrain the deformation of the matrix. Thus, the higher the volume fraction of coarse aggregate, the lower the CTE of corresponding concrete.

7 Conclusion

In this research, to combine time variability of early-age cement paste's CTE and randomness of aggregate's distribution, macro-scale has been divided into concrete meso-scale, mortar scale, cement paste scale, according to the scale law. Then, a specific REV for each scale is described by introducing stochastic parameters, and successfully realizes the connection between different scales using asymptotic expansion theory. Thus, a stochastic multi-scale model for CTE of early-age concrete is proposed.

A comparison study with experimental results and Rosen-Hashin bounds at mortar scale is conducted, which validate the effectiveness of this model proposed in this research, where, results of proposed model are in good agreement with experimental data, and close to or slightly higher than the Rosen-Hashin upper bound within permissible error.

Based on the computation results on mortar scale, a cross-scale to macro-scale study is performed, and three kinds of normally used representative aggregates are chose to investigate the influence of aggregate's type and volume fraction. Aggregate's type has important influence on CTE of concrete at early-age, where the CTE

of concrete with calcareous aggregate (limestone) is obviously lower than concrete with siliceous aggregate (quartzite), while concrete with igneous aggregate (granite) fall in between these two; besides, the higher the volume fraction of aggregate, the lower the CTE of corresponding concrete.

Admittedly, in the proposed model, mechanical and thermal properties of cement paste are obtained directly from fine experiments. However, it's expected that this completely cross-scale research from cement paste to macro structure of concrete can be effectively realized by advanced experimental observation techniques and the multi-scale modeling method, it shows that the proposed model can effectively estimate the CTE of concrete at early-age through taking the influence of material composition and configuration into consideration. Related studies are being carried on currently.

Acknowledgement

The research was financially supported by the National Basic Research Program of China (973 Program: 2011CB013800), and the National Natural Science Foundation of China (50908167 and 50838004), which are gratefully acknowledged.

References

- Abdulrazeg, A. A.; Noorzaei, J.; Khanehzaei, P.; Jaafar, M. S.; Mohammed, T. A.** (2010): Effect of temperature and creep on roller compacted concrete dam during the construction stages. *CMES: Computer Modeling in Engineering & Sciences*, vol. 68, no. 3, pp. 239-268.
- Amin, M. N.; Kim, J. S.** (2009): Simulation of the thermal stress in mass concrete using a thermal stress measuring device. *Cement and Concrete Research*, vol. 39, pp. 154-164.
- Azenha, M.; Faria, R.** (2009): Identification of early-age concrete temperatures and strains: Monitoring and numerical simulation. *Cement and Concrete Composites*, vol. 31, pp. 369-378.
- Ballim, Y.; Graham, P. C.** (2004): Early-age heat evolution of clinker cements in relation to micro-structure and composition implications for temperature development in large concrete elements. *Cement and Concrete Composites*, vol. 26, pp. 417-426.
- Bazant, Z. P.** (1970): Delayed thermal dilatations of cement paste and concrete due to mass transport. *Nuclear Engineering and Design*, vol. 14, no. 2, pp. 308-318.
- Bazant, Z. P.; Kaplan, M. F.** (1996): *Concrete at High Temperatures: Material Properties and Mathematical Models*. Longman (Addison-Wesley), London, Eng-

land.

Bohm, H. J.; Han, W.; Eckschlager, A. (2004): Multi-inclusion unit cell studies of reinforcement stresses and particle failure in discontinuously reinforced ductile matrix composites. *CMES: Computer Modeling in Engineering & Sciences*, vol. 5, no. 1, pp. 5-20.

Briffaut, M.; Benboudjema, F. (2011): A thermal active restrained shrinkage ring test to study the early age concrete behavior of massive structures. *Cement and Concrete Research*, vol. 41, pp. 56 – 63.

Cusson, D.; Hoogeveen, T. (2006): Measuring early-age coefficient of thermal expansion in high-performance concrete. *RILEM: Volume Changes of Hardening Concrete*, pp. 321–330.

Constantinides, G.; Ulm, F. J. (2004): The effect of two types of C–S–H on the elasticity of cement-based materials: results from nano-indentation and micromechanical modeling. *Cement and Concrete Research*, vol. 34, no. 1, pp. 67-80.

Chang, S. P.; Zhang, S. M. (2007): *Engineering geology Manual*, Fourth edition, Building Industry Press, Beijing, China.

Cui, J. Z.; Cao, L. Q. (1998): Finite element method based on two-scale asymptotic analysis. *Mathematica Numerica Sinica.*, vol. 20, no. 1, pp. 89-102.

Du, C. B.; Jiang, S. Y.; Qin, W.; Zhang, Y. M. (2011): Numerical analysis of concrete composites at the meso-scale based on 3D reconstruction technology of X-ray CT images. *CMES: Computer Modeling in Engineering & Sciences*, vol. 81, no. 3, pp. 229-247.

Feng, Y. P.; Cui, J. Z. (2004): Multi-scale analysis and FE computation for the structure of composite materials with small periodic configuration under condition of coupled thermo-elasticity. *International Journal for Numerical Methods in Engineering*, vol. 8, pp. 1879-1910.

Grasley, Z. C.; Lange, D. A. (2007): Thermal dilation and internal relative humidity of hardened cement paste. *Materials and Structures*, vol. 40, pp. 311–317.

Ilc, A.; Turk, G. (2009): New numerical procedure for the prediction of temperature development in early age concrete structures. *Automation in Construction*, vol. 18, pp. 849 –855.

Kesavan, S. (1979): Homogenization of elliptic eigenvalue problems I. *Applied Mathematics & Optimization*, vol. 5, no. 1, pp. 153-167.

Kesavan, S. (1979): Homogenization of elliptic eigenvalue problems II. *Applied Mathematics & Optimization*, vol. 5, no. 1, pp. 197-216.

Li, Y. Y.; Cui, J. Z. (2004): Two-scale analysis method for predicting heat transfer

performance of composite materials with random grain distribution. *Science in China (Series A)*, vol. 47, no. 1, pp. 101-110.

Maruyama, I.; Teramoto, A. (2011); Impact of time-dependant thermal expansion coefficient on the early-age volume changes in cement pastes. *Cement and Concrete Research*, vol. 41, pp. 380–391.

Noorzaei, J.; Bayagoob, K. H.; Abdulrazeg, A. A.; Jaafar, M. S.; Mohammed, T. (2009): Three dimensional nonlinear temperature and structural analysis of roller compacted concrete dam. *CMES: Computer Modeling in Engineering & Sciences*, vol. 47, no. 1, pp. 43-60.

Ozawa, M.; Morimoto, H. (2006): Estimation method for thermal expansion coefficient of concrete at early ages. *RILEM: Volume Changes of Hardening Concrete*, 331–339.

Rosen, B. W.; Hashin, Z. (1970): Effective thermal expansion coefficients and specific heats of composite materials. *International Journal of Engineering Science*, vol. 8, no. 2, pp. 157–173.

Sellevoid, E.; Bjøntegaard, O. (2006): Coefficient of thermal expansion of cement paste and concrete: mechanisms of moisture interaction. *Materials and Structures*, vol. 39, no. 9, pp. 809–815.

Siboni, G.; Benveniste, Y. (1991): A micromechanics model for the effective thermo mechanical behavior of multiphase composite media. *Mechanics of Materials*, vol. 11, pp. 107-123.

Schapery, R. A. (1968): Thermal expansion coefficients of composite materials based on energy principles. *Journal of Composite Materials*, vol. 2, no. 3, pp. 380–404.

Wang, T. M. (1997): *Crack control of engineering structures*. Building Industry Presss, Beijing, China.

Wyrzykowski, M.; Lura, P. (2013): Controlling the coefficient of thermal expansion of cementitious materials – A new application for superabsorbent polymers. *Cement and Concrete Composites*, vol. 35, pp. 49-58.

Yang, Z. Q.; Cui, J. Z.; Nie, Y. F.; Ma, Q. (2012): The second-order two-scale method for heat transfer performances of periodic porous materials with interior surface radiation. *CMES: Computer Modeling in Engineering & Sciences*, vol. 88, no. 5, pp. 419-442.

Yeon, J. H.; Choi, S. (2013): In situ measurement of coefficient of thermal expansion in hardening concrete and its effect on thermal stress development. *Construction and Building Materials*, vol. 38, pp. 306–315.

Zhu, B. F. (1999): *Temperature stress and temperature control of mass concrete*.

Electric Power Press, Beijing, China